Robotic Exploration Of Surfaces With A Compliant Wrist Sensor

MS-CIS-90-92
GRASP LAB 244

Pramath R. Sinha
Yangsheng Xu
Ruzena Bajcsy
Richard P. Paul

Department of Computer and Information Science
School of Engineering and Applied Science
University of Pennsylvania
Philadelphia, PA 19104-6389

December 1990

Robotic Exploration of Surfaces with a Compliant Wrist Sensor *

Pramath R. Sinha[†]   **Yangsheng Xu**[‡]   **Ruzena K. Bajcsy**
Richard P. Paul
General Robotics and Active Sensory Perception (GRASP) Laboratory
Department of Computer and Information Science
University of Pennsylvania
Philadelphia, PA 19104-6228

Abstract

This paper presents some results of an ongoing research project to investigate the components and modules that are necessary to equip a robot with exploratory capabilities. Of particular interest is the recovery of certain *material* properties from a surface, given minimal *a priori* information, with the intent to use this information to enable a robot to stand and walk stably on a surface that is unknown and unconstrained. To this end, *exploratory procedures* (*ep*'s) have been designed and implemented to recover penetrability, material hardness and surface roughness by exploring the surface using a compliant wrist sensor. A six degree-of-freedom compliant wrist sensor, which combines passive compliance and active sensing, has been developed to provide the necessary flexibility for force and contact control, as well as to provide accurate position control. This paper describes the compliant wrist and sensing mechanism design along with a hybrid control algorithm that utilizes the sensed information from the wrist to adjust the apparent stiffness of the end-effector as desired.

1 Introduction

Robotic systems are being increasingly applied to the areas of agriculture, underwater, mining, space exploration, and hazardous environments. In such applications, where the environment is quite unstructured, there is a need to equip robots with exploratory capabilities such that robots can actively explore and adapt to the unconstrained environment. The motivation for research on surface exploration, therefore, stems from the need to have a robotic system that actively explores the environment to recover some of its characteristic properties, and then applies this information to the successful execution of specified tasks.

The proposed framework for surface exploration is quite general and can be conceivably useful in a wide variety of applications - grasping, manipulation, material identification, and in the creation of physical models of the environment in direct or teleoperated tasks. In particular, however, we will address the issue of exploration to extract *material* properties from a given surface for the specific

purpose of legged locomotion. Much in the same way as humans walk on surfaces of different material properties, constantly evaluating the behavior of the terrain with their feet and making adjustments in the foot forces so that they do not slip, fall, or sink, we propose a device that serves both as a probe and a foot for a robotic system, and a methodology to identify the material parameters of the surfaces that the robot would encounter during locomotion. This issue has never really been investigated before since, in the design of most legged robots, it is assumed that the material properties, the geometry, and conditions of the environment are known *a priori* or are controllable (IJRR 1990). Concurrently with our work, some research has been done in the area by Krotkov (1990) emphasizing further the need to measure material properties from the terrain to improve the quality of legged locomotion in rugged terrain.

The first part of the paper discusses the proposed framework for exploration with reference particularly to legged locomotion. The second part of the paper discusses the design and implementation of a compliant wrist sensing mechanism which can be used for a variety of applications, not necessarily restricted to the specific task of surface exploration discussed here. This is the primary sensing device used in our experiments and even though we have really used it as an *ankle* on our foot (in the anthropomorphic sense), we refer to it as a *wrist* since it was originally built as one. The final section of the paper describes the system setup and implementation of our proposed *ep*'s to recover *material* properties from a surface, given minimal *a priori* information.

2 Proposed Framework for Surface Exploration

Our first objective was to identify the attributes that are needed to determine the stability of surfaces during standing or walking. A detailed description of our investigations into the attributes of interest can be found in (Bajcsy 1989; Sinha et al 1990). We examined some salient attributes of a wide variety of commonly encountered materials and compiled a list of distinguishing and measurable attributes. Guided by the goals of our application, we chose to define the structure of our environment by the attributes of penetrability, hardness, compliance, compressibility, deformability and surface roughness. This choice of attributes was also supported by a review of work in soil mechanics (Bowles 1970; Bolton 1979) which showed that these are the important properties which would determine the behavior of surfaces composed of soils and sands under forces exerted by a foot during legged locomotion.

This choice of attributes is considerably different from those of interest to researchers in the obvious areas of perception like vision and touch. The geometric properties and the shape of the surface, which are important considerations even in legged locomotion, are not the focus of this research. We would also like to be able to predict the physical behavior of the surface under the influence of certain forces. As mentioned by Krotkov (1990), contrary to the most commonly used modalities in active vision or touch research, the modality to recover material properties is obviously that of force/torque sensing through contact. The advantage of using such a scheme is that not only does the robot have a "feel" for the surface but the local geometry of the surface can be sensed as well.

At present, the framework we propose is that for stable stepping and walking in an unknown environment, it is necessary to recover the attributes of penetrability, hardness, compliance, compressibility, deformability and surface roughness. The relevance of these properties in legged locomotion is actually quite intuitive and is elaborated upon in the following sections. Further, these attributes must be recovered actively by "exploratory procedures" (*ep*'s) that are built in to the mobile robotic system.

2.1 Attributes and Exploratory Procedures

Under the paradigm of exploratory robotics and active perception, the concept of *ep*'s provides a solid framework for exploration and recovery of attributes - for details refer to our earlier work (Bajcsy 1989; Sinha 1990). By *ep* we mean a procedure that is salient to the recovery of a specific attribute of interest. From a review of most available testing methods from scientific and engineering fields other than Robotics, most methods seemed completely unsuitable for Robotics applications. For example, soil engineers do most of their testing by taking soil samples and measuring the properties with specially designed equipment. The methodology of our research, therefore, is to design exploratory procedures that will attempt to recover the specific attributes of interest from the environment. These *ep*'s are then to be implemented to recover the properties from the surface and use them to be able to walk in a more efficient manner.

We would also like to take advantage of the fact that during legged locomotion, the foot comes in contact with the terrain and exerts certain forces on it. The surface responds in a certain way by deforming and exerting reactive forces on the foot. If this behavior of the surface is monitored, the robot can use its foot during the contact stage as not only a device for locomotion but also as a probe to recover material properties that will help it to avoid sinking or slipping and make suitable adjustments in the control strategies of the leg–ankle–foot system.

2.1.1 Penetrability

In measuring the penetrability of a surface we are interested in determining whether the surface is penetrable or not. It would give the robot the ability to decide whether its foot would sink into a surface or be able to find a stable footing. This is particularly of interest in detecting materials like quicksand, mud or soft snow, the surfaces of which would not support the weight of the robot and cause the foot to sink.

The *ep* for penetrability is analogous to the penetration tests that are used to examine soil properties (Bowles 1970). Soil engineers usually press a sharp mechanical probe into the surface and measure the resistance to penetration of the probe into the surface. In the case of a robot foot, however, it is more important to determine *whether* the surface is penetrable or not, rather than *how* penetrable it is. If a surface merely deforms or gets compressed initially (like soft sand or soil, for example), but then offers a stable surface due to its compressive strength, then it is considered to be impenetrable.

Our *ep* for penetrability, therefore, is designed to push the foot against the surface with a specified force. If the foot sinks below the surface, beyond a specified limit of stability, then the surface is classified is penetrable. On the other hand if the surface is able to withstand the force exerted by the foot, before the stability limit is reached, the surface is classified as impenetrable and the *ep* for hardness and compliance can then be implemented.

2.1.2 Hardness and Compliance

In measuring the attributes of hardness and compliance, we are highlighting those characteristics of an impenetrable surface that determine how the surface will behave when the foot exerts forces normal to it while standing or walking. Hardness and compliance can be interpreted in a number of ways (Bajcsy 1989; Petty 1971). Our interpretation is that hardness is the resistance (measure of deformation) to a load when the surface is rigid, while compliance is the same property measured for deformable surfaces. The basic concept of the *ep* for hardness and compliance is based on this interpretation.

The knowledge of surface hardness and compliance along with a measure of penetrability is extremely important to evaluate the support offered to the foot by the terrain. This would enable the robot to avoid areas that might upset its balance as well as to adjust the forces it is exerting to gain a better foothold. The compliance of the terrain will also be helpful in determining the most energy efficient path along the terrain.

A viable way to measure hardness and compliance is to measure the resistance to a load as deformation in a compliant probe when it is pressed against a hard material with increasing pressure (Bajcsy 1984). In the *ep* for hardness and compliance, we propose that the foot (that is rigid, but mounted on to a compliant device) is pressed against the material surface and then moved into the surface with small increments. Deformation in the compliant device is measured with each movement. This *ep* gives a measure of the material hardness and compliance which is proportional to the rate of deformation in the device. In addition, for materials that are compressive, the rate of deformation gives a measure of the compressibility and the extent of the maximum deformation is a measure of the compressive strength of the materials.

In the execution of this *ep*, what the robot really measures is the stiffness of the environment, where the stiffness is proportional to the rate of deformation in the compliant device. In the discussion of the implementation of this *ep* in Section 4.3 , we use some simple lumped-parameter dynamic models to show why this assertion is more than just intuitive.

It should be obvious that the *ep*'s for both penetrability and hardness can be easily implemented in downward motion of the foot during locomotion. Both the *ep*'s can be employed as the foot touches the surface and exerts increasing forces on it.

2.1.3   Surface Roughness

The surface roughness is a measure of the tangential forces due to friction that result when two surfaces in contact slide against each other. It would be of utmost importance to measure the surface roughness of surfaces to determine the forces that a robot should exert while walking on it. The knowledge of the roughness of a surface would give a walking robot the ability to avoid slipping when walking from a very rough surface on to a very smooth and slippery surface. The measure of roughness will also determine the amount of traction the surface can provide to a moving robot thus improving its ability to find secure footholds and making it energy efficient.

The *ep* for surface roughness is very similar to the classical methods of measuring the coefficient of friction between the two surfaces. The *ep* is simply designed to perform relative lateral motion between a surface of known roughness (in our case, the foot) and the unknown surface, while keeping them forced into contact. The measurement of tangential forces generated when this *ep* is carried out will give us a measure of the surface roughness. Once again our goal is to be able to employ this *ep* and recover the roughness of the surface during the interaction of the foot with the surface during legged locomotion. This can be done when the foot is being used to propel the robot forward. The traction forces generated at the surface will give us a measure of the surface roughness.

We now describe the design and control of the compliant wrist sensing mechanism that is the primary sensor used in the implementation of the *ep*'s described above.

3   Passive Compliance and Active Sensing Mechanism

The first part of this section gives some background on the research done in the area of compliant mechanisms. The design of the compliant wrist sensing mechanism is described in the next part

and we conclude the section with a short description of the hybrid position/force control scheme implemented to control our system during the implementation of the *ep*'s discussed earlier.

3.1 Previous Research on Compliant Devices

When robots are used in operations where end effectors contact the environment, compliance is beneficial in allowing external constraints to modify the trajectory. Considerable attention has been directed to compliant motion of robot manipulators in this decade. We may categorize currently available compliant motion control techniques into two basic types. Firstly, active compliance is specified in the joint servo either by setting a linear relation between the force and displacement (or velocity and displacement) such as in impedance control (Hogan 1984), damping control (Whitney 1977), and stiffness control (Salisbury 1980), or by controlling force in certain degrees-of-freedom while controlling position in the others, such as in compliance control (Paul 1982), compliance and force control (Mason 1982), and hybrid control (Raibert and Craig 1981). Secondly, passive compliance is provided by a compliant element near the end-effector, usually incorporated into a wrist, a hand, or fingers. The most well known example is the Remote Center of Compliance (RCC) (Whitney and Rourke 1986), although many different versions have been developed in Japan (Takase et al 1974; Asada and Ogawa 1987), France (Reboulet and Robert 1986; Merlet 1987) West Germany (Dillmann 1982) and the USA (Cutkosky and Wright 1982; Bausch et al 1986).

There are fundamental problems with both techniques. For active compliance, the response rate is limited and an instability problem is observed in stiff environments. Therefore, passive compliance installed in the end-effector is desirable to reduce the overall system stiffness. Passive compliance also possesses other advantages such as accommodating geometric uncertainties and dimensional tolerances, reducing the high forces or moments usually caused by assembly or other contact operations, and avoiding costly electronic instrumentation normally required in precision tasks. In using passive compliance alone, however, the positioning capability of robot is degraded. Many researchers have tried to address these problems (Seltzer 1986; Kazerooni and Guo 1987; De Schutter 1987; Brussel et al 1981), but the need for a simple, economical and reliable solution still exists.

In this paper, we propose a passive compliance mechanism with six degrees-of-freedom compliance that is also capable of measuring the six degrees-of-freedom deflections within the device, that is, between the end-effector and robot wrist. Passive compliance is used to allow for relaxed tolerances and absorb sudden impact forces, as well as to accommodate the transition between the position and force control modes. The sensed deflection in the wrist is used for feedback control such that the entire robotic system is controllable. The compliance and sensing mechanism are described in the next part and the hybrid control scheme is detailed subsequently.

3.2 Design of the Compliant Wrist Sensing Mechanism

There are two plates, upper and lower, in the compliant wrist device. The lower plate is attached to the robot and the upper one is connected with the end-effector. A compliant, damped rubber structure is installed between the plates to provide passive compliance. The device provides similar compliance in and around all three axes in order to accommodate transitions and to absorb the kinetic energy as the robot makes contact with environment in any direction. The compliance mechanism of the device is shown in Figure 1.

The passive compliance mechanism is composed of different blocks so as to accommodate different types of operations and to allow for changes in the compliance mechanism without necessitating
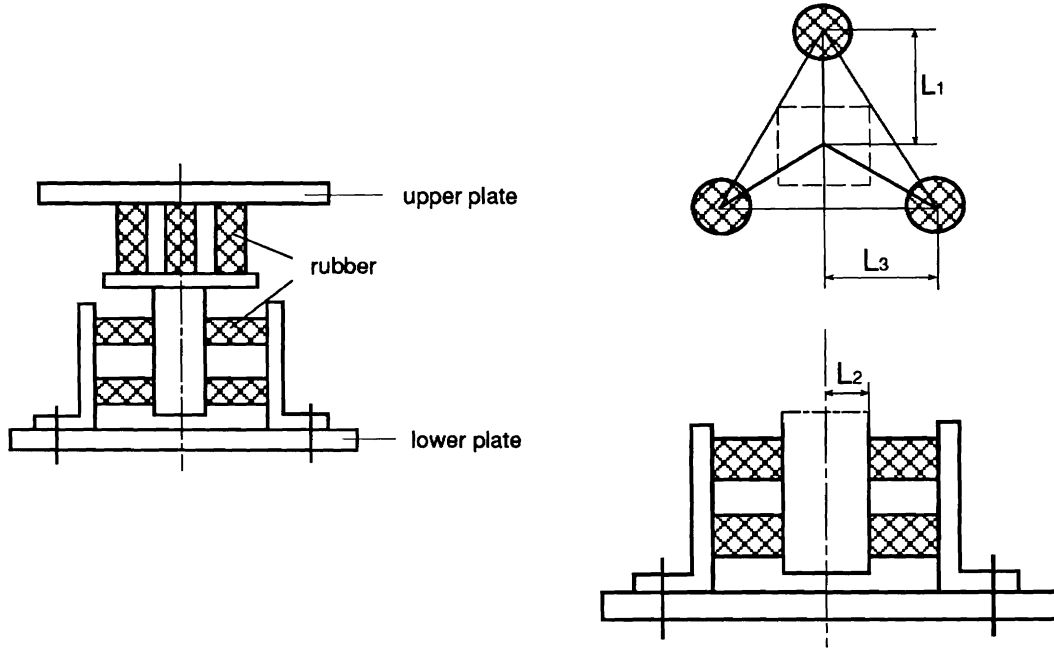
Figure 1: Different views of the passive compliance mechanism

a change in the sensing mechanism. Each block of the passive compliance mechanism is assembled from several single pieces of rubber. These pieces are commonly used as sandwich mounts for flex-bolts. The rubber element was chosen because the stiffness of rubber and its shape which yields reasonable stiffness in each direction. Also, from a stability analysis, some damping in the device is necessary as the damping ratio of the system is critical for system performance (Xu and Paul 1988). The rubber material in the device provides significant inherent damping.

An example of the block structure is shown in Figure 1. It consists of two portions: the upper one with three rubber elements in an equilateral triangle and the lower one with eight elements placed horizontally in the four sides of a cube connected to the lower part. The compliance in the upper part contributes mainly to the axial stiffness, and while the compliance in the lower part provides the lateral and torsional stiffnesses. Both parts contribute to the bending stiffness.

The design of the sensing mechanism is based on the mechanism sensitivity ellipsoid theory (Xu 1989). The design goal was to find a mechanism configuration around which the motion at the end-point had approximately equal sensitivity to the motion of each joint. In other words, it was required that for any given arbitrary displacement at the end-point of the mechanism all joints should exhibit approximately equal motions. The mechanism shown in Figure 2 can provide a nearly isotropic kinematic sensitivity. The linkage is arranged around a hypothetical cube as shown in Figure 3. A detailed discussion of the design based on the kinematic and dynamic ellipsoids may be found in (Xu 1989).

The sensing mechanism installed between these two plates is capable of measuring the six degrees-of-freedom relative motions of the upper plate with respect to the lower one. The sensing mechanism is formed by a serial linkage with a transducer at each of its six joints. The joint angular change is measured and then the position change in Cartesian space is computed to represent the six degrees-of-freedom deflections of the compliant wrist due to the external force during motion
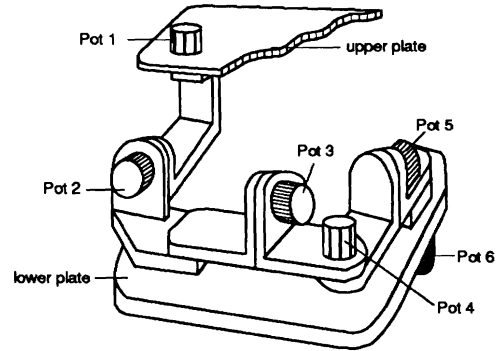
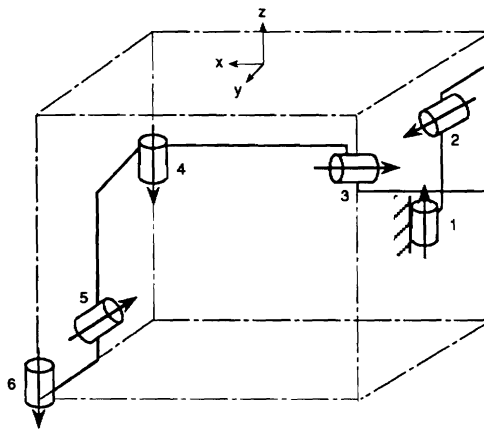Figure 2: Sensing Mechanism of the Wrist Sensor

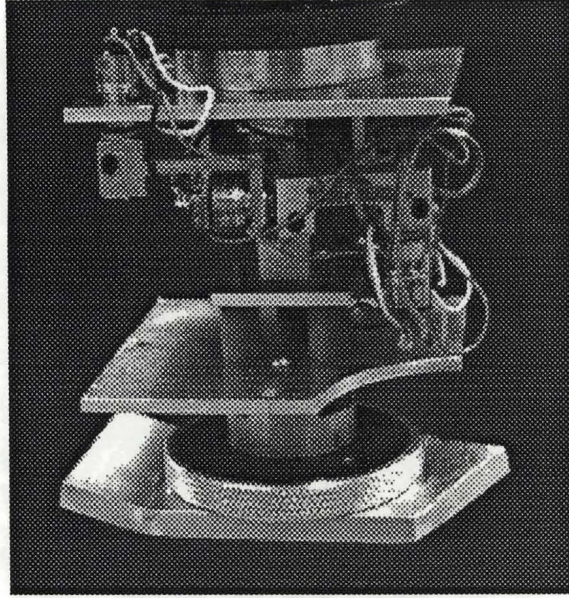Figure 3: Kinematic skeleton of the Sensing Mechanism

Figure 4: Compliant Wrist Sensor with Foot

or contact. The Cartesian deflections can thus be computed directly from the input joint data by means of direct kinematics. It was the simplicity of the direct kinematics that prompted the choice of a serial linkage as opposed to a parallel one.

For this particular design, the lateral stiffness is lower than in the other directions since the geometric error is normally corrected in this direction. The axial stiffness is stronger than that in bending and torsional directions for greater load capacity and minimum positioning error. The detailed technical specifications for the wrist and the values for stiffnesses in the device can be found in (Xu 1989). The maximum allowable workspace of the device is ±2.0in for translation in the lateral direction, and ±0.2in for that in axial direction. The maximum rotation in the bending direction is ±20 degrees, and that in torsional direction is ±30 degrees. The resolution of the device in translational direction is 0.01in and that in rotational direction is 0.25 degree.

We introduced passive compliance in each of six directions instead of the three or five directions found in most passive compliance devices. The reason is that the device is meant to be used not only to correct lateral and torsional errors in precision tasks but also to absorb kinetic energy when the robot manipulator encounters sudden forces upon making contact with the environment. In this way, the transition between force and position control is accommodated. The positioning capability will not be degraded because of active sensing and compensation in the feedback loop. A digitized image of the compliant wrist sensor is shown in Figure 4.

3.3 Hybrid Position/Force Control Scheme

To control the robot equipped with the compliant wrist a hybrid position/force control scheme was designed, with due consideration to the passive compliance in the system. The generalized surface on which the robot works can be defined in a constraint space having six degrees-of-freedom, with position constraints along the normals to this surface and force constraints along the tangents. These two types of constraints, force and position, partition the degrees-of-freedom of possible end-effector motions into two orthogonal sets, that must be controlled according to different control

8

strategies. The design of a hybrid control scheme was investigated under both cartesian space control and joint rate control. In this paper, we have chosen to describe the hybrid control scheme based on joint rate control, which is also the one that has been actually implemented. Further details and cartesian space control strategies can be found in some earlier work (Xu 1989; Xu 1990; Xu et al 1990).

Let us first consider the position control case when the robot moves in free space. The control scheme is designed to compensate for the positioning error due to the passive compliance in the wrist device by driving the robot in the opposite direction of the measured deflection in such a way that the overall stiffness is increased. Using the joint rate control representation, the desired joint motion to correct the position error is

$$\Delta\Theta_m = -\mathbf{J}_m^{-1}\Delta\mathbf{X}_w \tag{1}$$

where $\mathbf{J}_m$ is the manipulator Jacobian matrix, $\Delta\mathbf{X}_w$ is the generalized position error vector of the wrist and $\Delta\Theta_m$ is the corresponding joint motion in the robot. There are two ways to obtain the differential wrist displacement vector $\Delta\mathbf{X}_w$ composed of three position displacements and three orientation twists (relative to the initial position where the deflection is zero). Firstly, it can be extracted from the updated transformation matrix T_w of the wrist sensing mechanism. Secondly, these six differential deflections may also be calculated from the wrist mechanism Jacobian matrix $\mathbf{J}_w$ and $\Delta\Theta_w$ which both depend upon sensor joint angles:

$$\Delta\mathbf{X}_w = \mathbf{J}_w\Delta\Theta_w \tag{2}$$

For proportional control, the desired joint motion Θ_{des} is

$$\Theta_{des} = \Theta_{traj} + \Delta\Theta_m = \Theta_{traj} - \mathbf{J}_m^{-1}K_p\Delta\mathbf{X}_w \tag{3}$$

where K_p is the gain matrix and Θ_{traj} is the vector representing the required joint angles, supplied by a trajectory generator function.

In the force control case, where the end-effector is partially constrained by the workpiece, we use the compliant wrist as a sensor to detect the force exerted on the end-effector. For the degrees-of-freedom that force is being controlled, the sensed deflection is used to drive the manipulator in the same direction as the deflection of the wrist so that the desired stiffness is obtained.

Utilizing a joint rate control scheme, the desired stiffness K_d is related to the exerted force F_w on the wrist mechanism and the corresponding robot motion $\Delta\mathbf{X}_r$ by

$$F_w = K_d\Delta\mathbf{X}_r \tag{4}$$

Additionally, the exerted force F_w is related to the wrist deflection $\Delta\mathbf{X}_w$ by the physical stiffness of the device K_w

$$F_w = K_w\Delta\mathbf{X}_w \tag{5}$$

Substituting yields

$$\Delta\mathbf{X}_r = K_F\Delta\mathbf{X}_w \tag{6}$$

where K_F is a dimensionless ratio of stiffnesses

$$K_F = K_d^{-1}K_w \tag{7}$$

9

The desired joint angles Θ_{des} are thus represented by

$$\Theta_{des} = \Theta_{curr} + \Delta\Theta_m = \Theta_{curr} + \mathbf{J}_m^{-1} K_F \Delta\mathbf{X}_w \tag{8}$$

where Θ_{curr} represents the current joint angles. The position and force control algorithms are very similar and both contain a dimensionless gain term K_P or K_F but with different signs in front. The former represents the gain matrix controlling the amount of deflection we wish to compensate for in position control. The latter represents another gain matrix relating the natural stiffness of the end-effector to the effective stiffness of the system, which is to be controlled in the force control task. If complete compensation in all directions is required in position control, the gain K_P is an identity matrix. If the desired compliance level is just the natural compliance, K_w, of the wrist, the gain matrix K_F is again an identity matrix. Also note that the desired joint angles Θ_{des} depend on the specified joint angles Θ_{traj} in position control, while in the force controlled degrees-of-freedom the depend on the current joint angles Θ_{curr}. This can be understood by considering a situation in which a sudden force is exerted on the wrist and then it is immediately removed. For the force controlled degrees-of-freedom the deflections will be preserved if the desire was to comply completely to the force experienced. On the other hand, for the position controlled directions, the robot must move the end-effector back to the original position for complete compensation.

The hybrid control of a system, however, is normally executed with position and force control simultaneously. To perform this hybrid position/force control, we at first partition the measured deflection $\Delta\mathbf{X}_w$ into two sets: $\Delta\mathbf{X}_w^F$ corresponding to the force controlled component, and $\Delta\mathbf{X}_w^P$ in the remaining directions, corresponding to position control. For the given desired residual force $\mathbf{F}_d$, the corresponding residual deflection of the wrist device $\Delta\mathbf{X}_d$ can be evaluated by

$$\Delta\mathbf{X}_d = K_w^{-1}\mathbf{F}_d \tag{9}$$

where K_w is the physical stiffness of the wrist mechanism. Using the gain matrix, the desired differential motions of the end-effector corresponding to position and force control are

$$\Delta\mathbf{X}_P = K_P\Delta\mathbf{X}_w^P \tag{10}$$

$$\Delta\mathbf{X}_F = K_F(\Delta\mathbf{X}_w^F - \Delta\mathbf{X}_d) \tag{11}$$

Therefore, considering only force control, the desired joint motion of the end-effector tracks the force error represented by $\Delta\mathbf{X}_F$, based on the current motion.

$$\Theta_j = \Theta_{j-1} + \mathbf{J}_m^{-1}\Delta\mathbf{X}_F \tag{12}$$

Concurrently, when the position control is also considered, the end-effector motion must be modified by the deflection $\Delta\mathbf{X}_P$, and the final motion is

$$\Theta_j = \Theta_{j-1} + \mathbf{J}_m^{-1}\Delta\mathbf{X}_F - \mathbf{J}_m^{-1}\Delta\mathbf{X}_P \tag{13}$$

The applications of the compliant wrist using the above controller, are carried out on a PUMA 560 arm, and executed on a MicroVAX II using the RCI primitives of RCCL (Hayward 1984), which allows the software to directly command robot joint angles. The software package allows various parameters to be set, and also allows trajectory and wrist displacement data to be logged to a file for subsequent analysis. For simplicity, we will not discuss the effect of system parameters on the dynamic performance, a detailed discussion on which can be found in (Xu 1989).
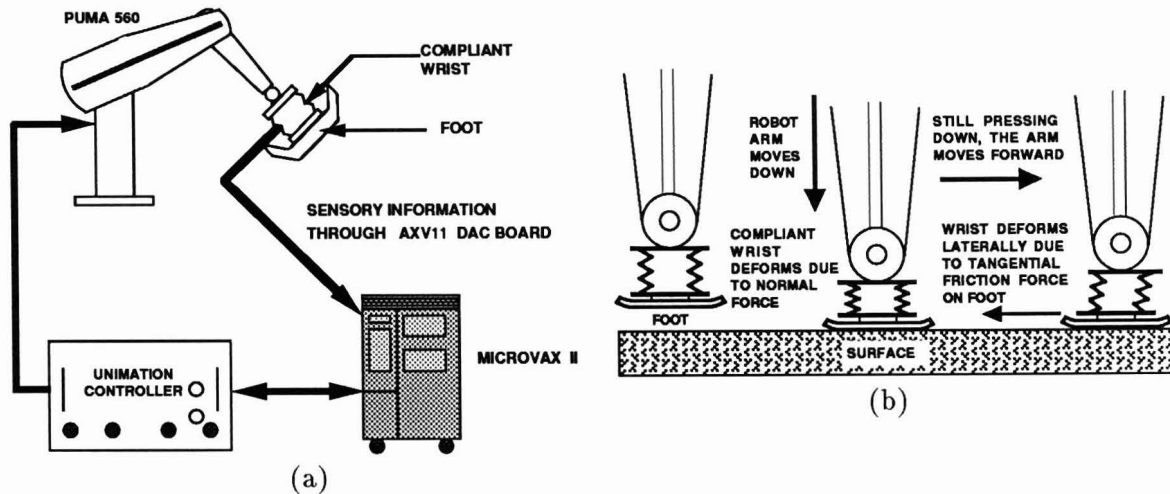
Figure 5: (a) System Setup (b) A Typical Run

4   Recovery of Attributes

To provide a robot the ability to sense the material properties of the surface while standing, or indeed walking on it, and to use it to improve the quality of legged locomotion is the ultimate goal of this research. Keeping this in mind and to test the framework proposed earlier, we have built a system and implemented the *ep*'s described in Section 2 with the intent to ultimately execute these *ep*'s on the fly, that is, while the robot is in motion and the foot is executing the movements for walking.

4.1   System Setup

The system setup is shown in Figure 5(a). The primary sensing mechanism is the compliant wrist sensor that has been described in the previous sections. The base of the compliant wrist is mounted on the PUMA 560 arm and our prototype foot has been mounted on the other end of the wrist. What we have here is the leg–ankle–foot system being represented by the Puma arm–compliant wrist–foot system. The design of the foot is quite intuitive and we have just built a simple device that looks like a short ski. The foot is made of aluminum and the bottom surface (the one that interacts with the environment) is a well-machined metal surface. The dimensions of the foot are roughly (2.5in X 5in X .25in).

While carrying out a typical implementation of the *ep*'s described above, the robot arm pushes down on the surface to execute the *ep*'s for penetrability, hardness and compliance (see Figure 5(b)). The compliant wrist deforms in a direction normal to the surface due to the resultant normal forces. These deformations and the distance moved by the arm are recorded to give a measure of the penetrability, hardness and compliance. The *ep* for surface roughness is then employed. Now, while keeping the wrist pushed against the surface with a constant force, the arm is moved relative to the surface, thus sliding the foot over it. This causes the wrist to deform laterally in a direction opposite to the motion of the arm. This deformation is due to the tangential force of friction on the foot caused by roughness of the surface. Therefore, a measure of this lateral deformation gives a measure of the surface roughness.

In the following sections, we would like to particularly discuss the attributes of penetrability,
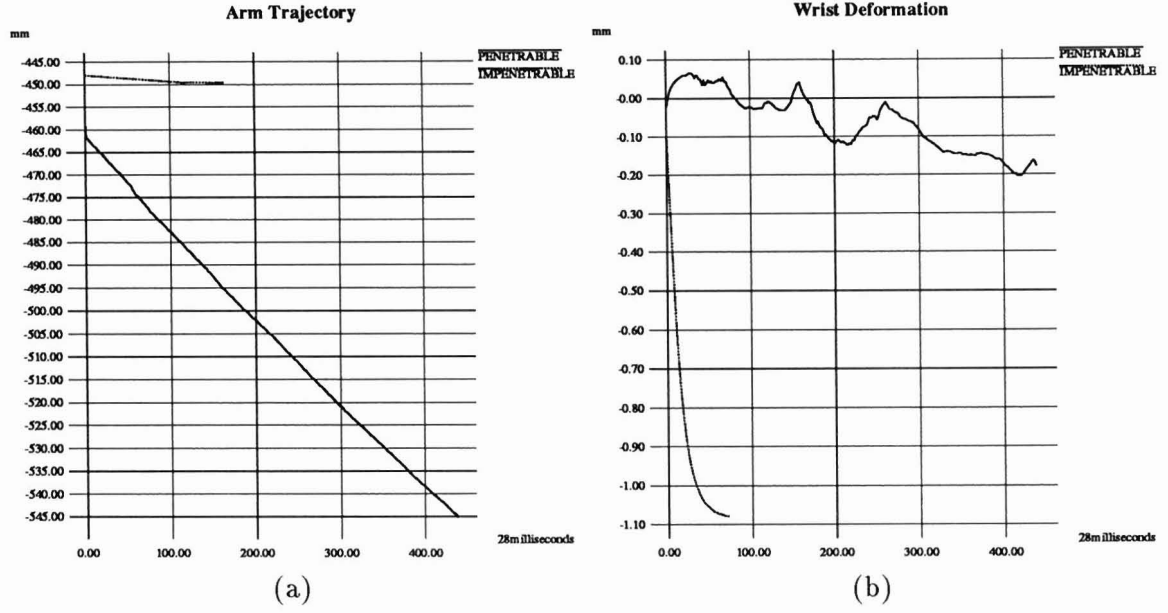
11

Figure 6: Measurement of Penetrability (a) Plot of arm end-point position (in mm) vs time (1 unit = 28 milliseconds) (b) Plot of deformation in the wrist (in mm) due to normal force vs time (1 unit = 28 milliseconds)

hardness and surface roughness because those are the three mechanical properties that we have so far succeeded in recovering.

4.2   Penetrability

This *ep* involves pressing down on the surface till a certain maximum normal deformation is measured in the wrist (which means that the surface is impenetrable, and can support the weight exerted by the foot), or till the arm has moved too far down (which means that surface is penetrable and the foot will sink into the surface). In the actual implementation, the maximum allowable normal deformation will be the equivalent to the deformation corresponding to the maximum normal force that the foot will exert on the surface. How far the arm should move down will be dictated by the limit on the sinkage of the foot, such that robot does not become unstable and fall. For our implementation of this *ep*, we have restricted the maximum normal deformation to be about -1.1mm (which corresponds to a normal force of about 6 lbs) and the maximum distance moved by the arm to about 80mm. If we find, by monitoring the distance moved down by the arm and the amount of deformation in the wrist, that the wrist deformation is very small compared to the large distance moved down by the arm, we classify the material as penetrable. Hence, penetrability is measured as a combination of arm trajectory and wrist deformation in a given time interval.

Some results from the *ep* for penetrability are shown in Figure 6. In the case of the penetrable surface, there is hardly any deformation in the wrist, in fact, only about -0.2mm (solid line in Figure 6(b)), even after the arm moves down the allowed 80mm (solid line in Figure 6(a)). On the other hand, for the impenetrable case, the arm moves down a very short distance (dotted line in Figure 6(a)) and most of the downward motion shows up as deformation in the wrist (dotted line in Figure 6(b)). Also, in the penetrable case the duration of the *ep* is very short as the wrist deforms rapidly and reaches the maximum permitted value.
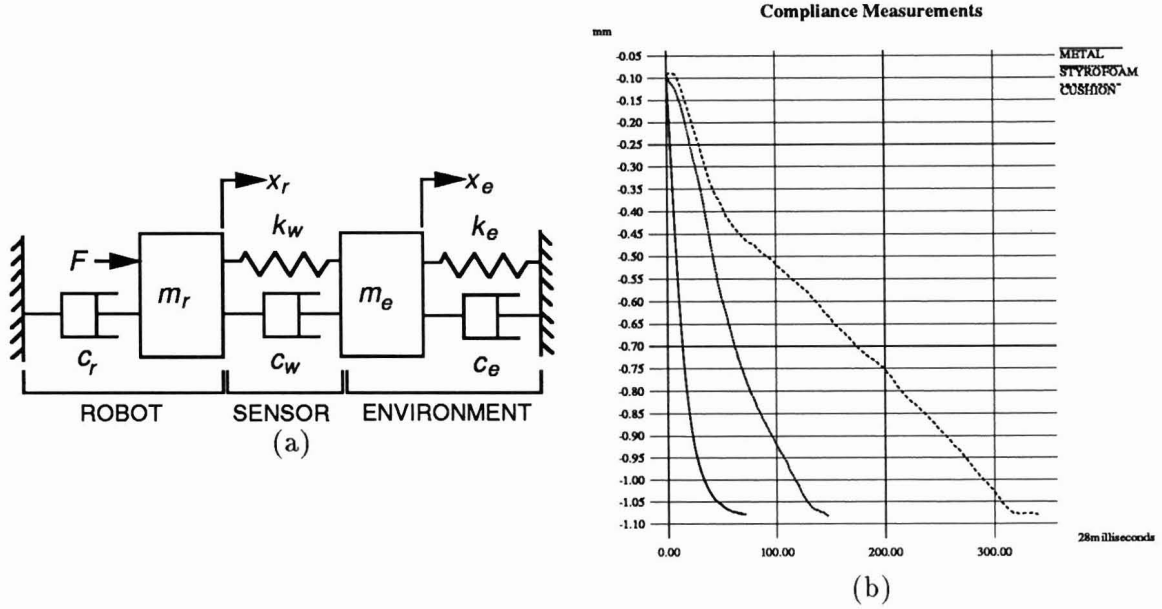
12

Figure 7: (a) Model of system for measurement of hardness (b) Plot of deformation in the wrist (in mm) due to normal force vs time (1 unit = 28 milliseconds)

4.3 Hardness

Our system can be modeled as a simple lumped-parameter dynamic model shown in Figure 7(a). We assume that the dynamics of the environment are adequately modeled by a second order dynamic model. Let us consider the arm to be a rigid body with no vibrational modes and model it as a mass with a damper to the ground. The mass m_r represents the effective moving mass of the arm. The viscous damper c_r gives the appropriate rigid body mode to the arm. The compliant wrist sensor connects the arm and the environment with some compliance - it has stiffness k_w and damping c_w. The environment is represented by a mass m_e and has a stiffness k_e and damping c_e. The state variables x_r and x_e measure the positions of the arm and environment masses, respectively. The actuator is represented by the input force F. The contact force F_c and the wrist deformation x_w are related as follows:

$$F_c = k_w x_w \tag{14}$$
$$\text{also,} \quad x_w = x_r - x_e \tag{15}$$
$$\text{therefore,} \quad F_c = k_w(x_r - x_e) \tag{16}$$

The governing equations for this system are:

$$m_r \ddot{x}_r + k_w(x_r - x_e) = F - c_r \dot{x}_r - c_w(\dot{x}_r - \dot{x}_e) \tag{17}$$
$$m_e \ddot{x}_e + k_w(x_e - x_r) + k_e x_e = c_w(\dot{x}_r - \dot{x}_e) - c_e \dot{x}_e \tag{18}$$

For the implementation of our *ep* for hardness, we can reasonably assume that $\ddot{x}_r = \dot{x}_e = c_r = c_w = c_e = 0$ for the velocities and frequencies of this *ep* are well within the dynamic range of the system. Therefore, the above equations reduce to:

$$k_w(x_r - x_e) = F \tag{19}$$
$$k_w(x_e - x_r) + k_e x_e = 0 \tag{20}$$

13

Substituting for x_e in Equation (20), using Equation (15) and differentiating, we get:

$$k_e = \frac{k_w \dot{x}_w}{\dot{x}_r - \dot{x}_w} \qquad (21)$$

Since k_w is a known constant obtained by calibration, and $\dot{x}_r$ is the constant commanded robot velocity, the environment stiffness, k_e, that the ep for hardness and compliance tries to measure, is just a function of $\dot{x}_w$, the rate of deformation of the wrist. Since $\dot{x}_w \leq \dot{x}_r$ at all times, we can say that the higher the value of $\dot{x}_w$, the greater is the hardness or stiffness of the system and vice-versa.

In our system, the ep for hardness involves moving down the arm such that the foot is pressed into the surface at a constant rate till the normal deformation experienced by the wrist is about -1.1mm (which corresponds to a normal force of about 6 lbs). It is first determined if the foot has encountered the surface. Then the foot is slowly pushed against the surface at a constant velocity ($\dot{x}_r$). The deformation history of the wrist is examined from the point the ep begins till it ends when the wrist is experiencing a normal deformation of about -1.1mm. The steeper the slope ($\dot{x}_w$) of the normal deformation versus time curve, the harder is the material.

The results from the ep for hardness measurements is shown in Figure 7(b). The slope of the deformation versus time plot is clearly the steepest for the metal surface. The Styrofoam surface is less hard, however, the curve is still mostly linear. In the case of the softer cushion, while the slope is clearly the least, the curve does not stay linear.

The interpretation of the changing slopes of these curves will help us in recovering attributes related to compliance, compressibility and deformability. These curves are actually analogous to load-sinkage curves that recover soil properties. This ep could thus be useful in measuring soil properties and its results could be interpreted to examine the behavior of soils. However, the precise basis of such interpretations is still being investigated.

4.4 Surface Roughness

The lumped-parameter model of the last section is modified for the measurement of surface roughness as shown in Figure 8(a). The surface roughness generates the tangential friction force F_f at the interface of the wrist sensor and the surface (in our case, the interface is the foot). Now, the friction force, F_f, is the same as the contact force, F_c, therefore, using Equation (14):

$$\text{since,} \quad F_f = F_c \qquad (22)$$
$$F_f = k_w x_w \qquad (23)$$

To measure the tangential force in order to obtain a measure of the surface roughness, therefore, all the robot needs to do is to measure the deformation, x_w, in the wrist sensor. In the implementation of the ep for surface roughness, the robot records the wrist deformations, x_w, in the direction opposite to the direction of lateral motion. This deformation is actually perpendicular to the deformation due to the normal force measured in the ep for hardness. In our experiments, the robot also adjusts, according to the hardness of the material, the normal force with which the foot is pressed against the surface and laterally moved along it.

The results of our ep for surface roughness are shown in Figure 8(b). The solid line denoting the normal force is really a plot of the deformations due to the normal force in the wrist. The flat part of that curve corresponding to a deformation of about -0.4mm signifies the constant normal force of about 2 lbs maintained during the sliding motion of the foot over the surface. The two curves above the x-axis are the plots of tangential deformations due to frictional forces encountered during the ep.
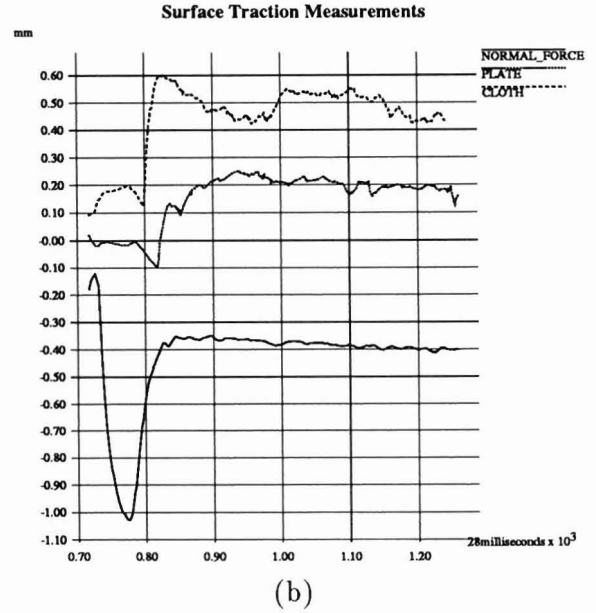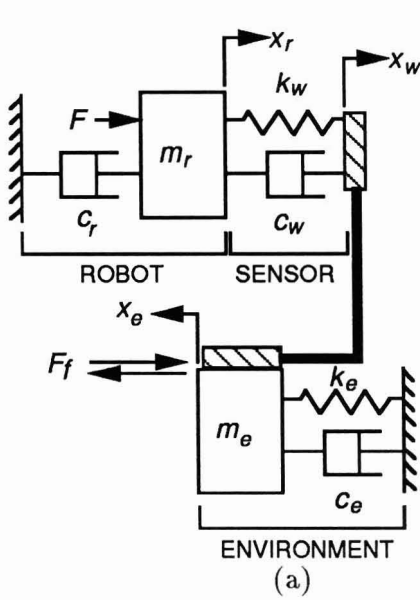
Figure 8: (a) Model of system for measurement of surface roughness (b) Plot of tangential and normal deformations (in mm) vs time (1 unit = 28 milliseconds) during surface roughness measurements

The lower of the two curves shows the wrist deformation corresponding to the surface roughness of a smooth plate. There is a constant deformation (corresponding to x_w in Equation (23)) of about 0.2mm. The curve at the top of Figure 8(b) shows the wrist deformation corresponding to the surface roughness of the plate covered by a rough cloth. In this case, the tangential forces are larger for the same normal force, due to the increased roughness of the surface, and as a result, the deformation, x_w, is larger, about 0.5mm. We have chosen an example where the material hardness is constant but the surfaces have different roughness properties. This shows conclusively that the robot is able to distinguish between surfaces of different roughness.

5   Conclusions

The ability to measure and sense the variation in the material properties of different surfaces is indispensable to mobility of robots in unstructured environments. To ensure that a robot does not slip and fall or sink and get stuck when standing or walking on a surface, the robot needs to measure the characteristic properties of the surface and continuously or periodically apply this information to adjust the forces it exerts on the surface during standing or walking.

With this in mind, we have succeeded in designing and implementing ep's to recover the penetrability, hardness and surface roughness characteristics of a surface. Current research is directed at investigating the mechanics of the foot–terrain interaction in order to better understand the connection between the material properties of the terrain and control strategies to be employed during legged locomotion. Ultimately, we would also like to account for variations in the geometry of the surface and, for example, also predict the stability of surfaces that are composed of rocks or pebbles.

We have also described the design and development of a compliant wrist sensor that incorpo-

15

rates passive compliance and active sensing. A hybrid position/force control algorithm has been proposed to control a robotic system equipped with such a sensor. While we are currently investigating the use of this device in the manufacturing and the telerobotic environments, in this paper we have described one particular area of application - the exploration of surfaces to extract material properties for use in robot locomotion.

References

Asada, H., and Ogawa, K. 1987 (March–April, Raleigh, NC). On the Dynamic Analysis of a Manipulator and its End-Effector Interacting with the Environment. *Proceedings of the IEEE International Conference on Robotics and Automation.* New York, NY: IEEE, pp. 751–756.

Bajcsy, R. 1984. What can we learn from One Finger Experiments ? In M. Brady and R.P. Paul (eds): *Robotics Research: The First International Symposium.* Cambridge, MA: MIT Press, pp. 509–528.

Bausch, J. J., Kramer, B. M., and Kazerooni, H. 1986. The Development of Compliant Tool Holders for Robotic Deburring. In F. Paul and K. Youcef-Tomi (eds): *Robots: Theory and Applications. Proceedings of ASME Winter Annual Meeting,1986,* pp. 79–89.

Bolton, M. 1979. *A Guide to Soil Mechanics.* John Wiley & Sons.

Bowles, J.E. 1970. *Engineering Properties of Soils and their Measurement.* McGraw-Hill Book Company.

Bajcsy, R., and Sinha, P.R. 1989 (December, New Delhi, India). Exploration of Surfaces for Robot Mobility. *Proceedings of the Fourth International Conference on CAD, CAM, Robotics and Factories of the Future.* New Delhi, India: Tata McGraw-Hill.

Brussel, H.V., Thielman, H., and Simons, J. 1981 (Tokyo, Japan). Further Developments of the Active Adaptive Compliant Wrist (AACW) for Robot Assembly. *Proceedings of the 11th International Symposium on Industrial Robots,* pp. 377–384.

Cutkosky, M.R., and Wright, P.K. 1982 (June, Paris, France). Position Sensing Wrists for Industrial Manipulators. *Proceedings of the 12th International Symposium on Industrial Robots.*

Dillmann, R. 1982 (November, Stuttgart, Germany). A Sensor Controlled Gripper with Tactile and Non-Tactile Sensor Environment. *Proceedings of the 2nd International Conference on Robot Vision and Sensory Controls.*

Hayward, V. 1984. *RCCL User's Guide.* edited for CVaRL by John Lloyd.

Hogan, N. 1984. Impedance Control of Industrial Robots. In *Robotics and Computer Integrated Manufacturing.* Elmsford, NY: Pergamon Press, pp. 97–113.

IJRR. 1990. Special Issue on Legged Locomotion. *The International Journal of Robotics Research.* Cambridge, MA: MIT Press, (9)2.

Kazerooni, H., and Guo, J. 1987 (March–April, Raleigh, NC). Direct-Drive, Active Compliant End-effector. *Proceedings of the IEEE International Conference on Robotics and Automation.* New York, NY: IEEE, pp. 758–766.

Krotkov, E. 1990 (September, Philadelphia, PA). Active Perception for Legged Locomotion: Every Step is an Experiment. *Proceedings of the Fifth IEEE International Symposium on Intelligent Control.*

Mason, M. 1982. Compliance and Force Control for Computer Controlled Manipulators. In M. Brady et al (eds): *Robot Motion: Planning and Control.* Cambridge, MA:

MIT Press, pp. 373–403.

Merlet, J-P. 1987 (March–April, Raleigh, NC). C-surface Applied to the Design of an Hybrid Force-Position Robot Controller. *Proceedings of the IEEE International Conference on Robotics and Automation.* New York, NY: IEEE.

Petty, E.R. 1971. Hardness Testing. In *Techniques of Metals Research.* John Wiley & Sons, 5(2):157–222.

Paul, R.P., and Shimano, B. 1982. Compliance and Control. In M. Brady et al (eds): *Robot Motion: Planning and Control.* Cambridge, MA: MIT Press, pp. 403–417.

Paul, R.P., and Xu, Y. 1990. The Implementation of Hybrid Control in the Presence of Passive Compliance. In H. Miura and S. Arimoto (eds): *Robotics Research 5.* Cambridge, MA: MIT Press, pp. 9–16.

Raibert, M.H., and Craig, J.J. 1981. Hybrid Position/Force Control of Manipulators. *ASME Journal of Dynamics Systems, Measurement, and Control.* 102:126–133.

Reboulet, C., and Robert, A. 1986. Hybrid Control of a Manipulator with an Active Compliant Wrist. In O.D. Faugera and G. Giralt (eds): *Robotics Research : The Third International Symposium.* Cambridge, MA: MIT Press, pp. 237–242.

Salisbury, J.K. 1980 (December, Albuquerque, NM). Active Stiffness Control of a Manipulator in Cartesian Coordinates. *Proceedings of the 19th IEEE Conference on Decision and Control,* pp. 87–97

Sinha, P.R., Bajcsy, R.K., and Paul, R.P. 1990 (July, Ibaraki, Japan). How Does a Robot Know Where to Step ? Measuring the Hardness and Roughness of Surfaces. *Proceedings of the IEEE International Workshop on Intelligent Robots and Systems '90 (IROS '90),* pp. 121–125.

De Schutter, J. 1987 (March–April, Raleigh, NC). Compliant Robot Motion Control Methods for Rigid Manipulators based on a Generic Scheme. *Proceedings of the IEEE International Conference on Robotics and Automation.* New York, NY:IEEE, pp. 1060–1065.

Seltzer, D.S. 1986. Compliant Robot Wrist Sensing for Precision Assembly. In F. Paul and K. Youcef-Tomi (eds): *Robots: Theory and Applications. Proceedings of ASME Winter Annual Meeting, 1986,* pp 161–168.

Takase, K., Inoue, H., Sato, K., and Hagiwara, S. 1974 (November, Tokyo, Japan). The Design of an Articulated Manipulator with Torque Control Ability. *Proceedings of the Fourth International Symposium on Industrial Robots,* pp. 261–270.

Whitney, D.E. 1977 (June). Force Feedback Control of Manipulator Fine Motions. *ASME Journal of Dynamic Systems, Measurement and Control,* pp. 91–97.

Whitney, D.E., and Rourke, J.M. 1986. Mechanical Behavior and Design Equations for Elastomer Shear Pad Remote Center Compliance. *ASME Journal of Dynamic Systems, Measurement, and Control,* 108:223–232.

Xu, Y., and Paul, R.P. 1988. On Position Compensation and Force Control Stability of a Robot with a Compliant Wrist. *Proceedings of the IEEE International Conference on Robotics and Automation.* New York, NY: IEEE, pp. 1173–1178.

Xu, Y., Paul, R.P., and Corke, P. 1990. Hybrid Position Force Control of a Robot Manipulator with an Instrumented Compliant Wrist. In V. Hayward and O. Khatib (eds): *Experimental Robotics 1.* Springer-Verlag, pp. 244–270.

Xu, Y. 1989. *Compliant Wrist Design and Hybrid Position/Force Control of Robot Manipulators.* MS-CIS-89-67, GRASP Lab 193. Philadelphia, PA: University of Pennsylvania, GRASP Lab, Department of Computer and Information Science.